NATIONAL ADVISORY COMMITTEE FOR AERONAUTICS

TECHNICAL NOTE 4405

FREE-FLIGHT INVESTIGATION TO DETERMINE THE DRAG OF FLAT- AND VEE-WINDSHIELD CANOPIES ON A PARABOLIC FUSELAGE WITH AND WITHOUT TRANSONIC INDENTATION BETWEEN MACH NUMBERS OF 0.75 AND 1.35

By Walter L. Kouyoumjian and Sherwood Hoffman

Langley Aeronautical Laboratory
Langley Field, Va.

Washington
September 1958

B

NATIONAL ADVISORY COMMITTEE FOR AERONAUTICS

TECHNICAL NOTE 4405

FREE-FLIGHT INVESTIGATION TO DETERMINE THE DRAG OF FLAT- AND VEE-WINDSHIELD CANOPIES ON A PARABOLIC FUSELAGE WITH AND WITHOUT TRANSONIC INDENTATION BETWEEN MACH NUMBERS OF 0.75 AND 1.35

By Walter L. Kouyoumjian and Sherwood Hoffman

SUMMARY

A free-flight investigation was conducted between Mach numbers of 0.75 and 1.35 to determine the effects on model total drag and pressure drag of (a) canopy location (along a parabolic body of revolution), (b) canopy windshield shape, (c) canopy fineness ratio, and (d) transonic-area-rule indentation.

The results of the investigation indicated that moving a 63° swept-back flat-windshield canopy rearward, from near the body nose to the maximum body diameter location, increased the model drag coefficients at transonic and low supersonic speeds. Changing to a vee-shaped windshield resulted in a negligible change in drag coefficient compared with that for the flat-windshield canopy. When the canopy fineness ratio was changed from 7.00 to 4.50 by shortening the canopy afterbody shape, the drag coefficients obtained for the short canopy were appreciably higher than those for the long canopy. The transonic-area-rule indentation proved effective in decreasing the pressure drag of all the canopy-fuselage combinations investigated to values within 10 percent of the pressure drag obtained for the basic parabolic body alone near a Mach number of 1.00. The effectiveness of the transonic-area-rule indentation decreased with increasing flight Mach number. Comparison of the theoretical and experimental pressure drag coefficients for approximately half of the number of canopies investigated indicated that the area-rule theory predicts the order of magnitude of the pressure drag and the qualitative difference in pressure drag due to the configuration modifications at transonic and low supersonic speeds.

INTRODUCTION

The present investigation was conducted to determine the drag characteristics of several canopy-body combinations at transonic speeds.

Other investigations of canopy-body combinations are presented in references 1 and 2. The flight Mach number range for the present investigation was from 0.75 to 1.35 and the Reynolds number per foot varied from 4.5×10^6 to 9.5×10^6 over the flight Mach number range. The basic fuselage used in this investigation was a smooth parabolic body of revolution with a fineness ratio of 10 and with the maximum diameter located at the 40-percent body station. The canopies were designed to investigate some effects of windshield shape, canopy length, and canopy location on the drag of fuselages with and without transonic-area-rule indentations. The canopies investigated consisted of flat-windshield canopies having equivalent body fineness ratios of about 7.00 and 4.50 and a vee-windshield canopy having an equivalent body fineness ratio of about 7.00. These fineness ratios are referred to as nominal fineness ratios for the purpose of indentification only since the actual canopy equivalent body fineness ratio changed slightly (table I) when the canopy position was varied and the fuselage indented.

The models that were flight tested without area-rule indentation had the same basic parabolic fuselage shape, whereas the models that were indented according to the area rule were contoured symmetrically for a Mach number 1.00 indentation to have the same cross-sectional area distribution and volume as the basic body alone. Although the canopy locations and shapes were varied, the indented models allow a comparative evaluation of the local interference effects on pressure drag at transonic speeds.

SYMBOLS

A	cross-sectional area, sq in.
a	acceleration, tangent to flight trajectory, g units
C_D	total drag coefficient based on a fuselage reference area of 19.63 sq in.
ΔC_D	pressure drag coefficient (Total drag coefficient at supersonic speeds - Total drag coefficient at $M_\infty = 0.8$)
r_c	canopy radius coordinate, in.
g	acceleration due to gravity, ft/sec^2
l	length of fuselage forebody, in.
M_∞	free-stream Mach number

S	reference area (19.63 sq in.)
W	weight of model, lb
x	longitudinal distance coordinate measured from tip, in.
y_c	canopy center-line reference coordinate, in.
y_r	fuselage radius coordinate, in.
q	dynamic pressure, lb/sq in.
γ	flight-path angle, deg

MODELS

A total of 10 canopy-fuselage models plus one basic body alone were tested during this investigation. Table I presents a summary of the 10 models and includes the position of the canopy-fuselage intersection in terms of the forebody length, x/l. The fuselage and canopy coordinates for all 11 models are presented in tables II and III. Figure 1(a) presents a general sketch of the basic body, including the stabilizing fins. The basic body was composed of two parabolas of revolution which were joined at the 40-percent station. The total length of the basic body (excluding fins) was 50 inches and the maximum body diameter at the 40-percent station was 5 inches. Figures 1(b) and 1(c) show the details of the flat-windshield and vee-windshield canopies, respectively. The canopies were divided into three groups: the first two groups were the flat-windshield canopies with nominal fineness ratios of 7.00 and 4.50; the third group consisted of the vee-windshield canopy with a nominal fineness ratio of 7.00. The actual canopy fineness ratios (table I) were obtained from equivalent bodies of revolution that had the same cross-sectional area distributions as the exposed canopies measured perpendicular to the fuselage center lines of the models tested.

The basic cross section of the canopies used was a circular arc, the locus of the centers of which was defined by the distance y_c measured from a canopy base reference line. The canopies used in the investigation were all patterned from the basic canopy. The solid core of the canopy was hollowed sufficiently to allow the canopy to touch the fuselage surface at the canopy foremost and rearmost points. Therefore, the location of the canopy base reference line was lowered and rotated because the canopy was positioned on the fuselage surface; and the distance between the fuselage surface and the fuselage center line diminished whereas the canopy coordinates remained constant. The individual

canopies were faired to the fuselage by dropping vertical lines from the canopy maximum width to the fuselage surface; for the indented models, the volume added by this method of fairing was considered and added to the volume of the fuselage to be removed. The flat-windshield canopy was obtained by cutting the basic canopy by a plane inclined 63° from the (vertical) Y-axis and intersecting the canopy at a point just before the canopy maximum radius coordinate. The vee-windshield canopy was obtained by passing two cutting planes through the basic canopy so that the planes were at an angle of 45° with the locus of canopy radius centers and skewed at an angle of 28.4° from the horizontal. The intersection of the two cutting planes was a straight line inclined from the vertical by 61.6° and faired into the canopy body with a smooth curve. The short canopy (flat, with a fineness ratio of 4.50) had the same windshield shape and frontal area as the long canopy, inasmuch as the afterbody of the long canopy was shortened to give the final profile for the short canopy.

Figure 2 presents photographs of a typical nonindented fuselage model and also a typical indented fuselage model. Figure 3 shows close-up photographs of all the canopy-fuselage models tested during the investigation. Figure 4 presents a comparison of the cross-sectional area distributions normal to the fuselage axis of all the models.

TESTS

The models were flight tested at the Langley Pilotless Aircraft Research Station at Wallops Island, Va. Each of the models was boosted to maximum flight velocity by a fin-stabilized 65-inch HVAR motor. A photograph of the booster motor and a typical model on a rail launcher prior to firing is shown in figure 5.

The models were ballasted to trim out at very low trim lift coefficients or approximately at zero lift. The experimental data for this investigation were taken from ground tracking radar by using a CW Doppler radar unit (and corrected for winds aloft) for velocity and a modified SCR-584 radar unit for trajectory measurements. Atmospheric conditions and winds aloft were measured at the time of each flight by balloon-carried rawinsonde.

DATA REDUCTION AND ANALYSIS

The total drag coefficient for each model was computed, during the decelerating portion of each flight, from the relation

$$C_D = -\frac{W}{gqS}(a + g \sin \gamma)$$

where the acceleration a was obtained by differentiating the velocity-time curve of the CW Doppler radar unit. The values of q and γ were obtained from measurements of tangential velocity and atmospheric conditions along the trajectory. The accuracy of the total drag coefficient (based on the fuselage maximum cross-sectional area) was estimated to be within ±0.005 at supersonic speeds and within ±0.01 at subsonic and transonic speeds. The Mach numbers were determined within ±0.005 for the flight range. The experimental drag-rise coefficients ΔC_D were defined as the difference between the total drag coefficient and friction drag coefficient at corresponding Mach numbers. The friction drag through the Mach number range was determined by adjusting the subsonic drag level of each model for Reynolds number effect by using the equations of Van Driest (ref. 3). A rather prominent joint existed where the fuselage tip joined the fuselage. (See fig. 2.) It was assumed that the boundary layers over the fuselage and canopies were altogether turbulent, being fixed by this joint, and that transition occurred at the 50-percent-chord station for the fins. No adjustments were made for the base drag coefficient of the models. Reference 4 indicates that, for afterbodies similar to those used in this investigation, the base drag level is of the order of accuracy of the drag measurements and can be neglected.

The theoretical pressure drag coefficients were computed for models A, B, C, E, G, and I by using the supersonic area rule of reference 5. The procedure is described in reference 6, and reference 7 provides information as to the convergence of the Fourier series used in the computations. Since the models with canopies were unsymmetrical, it was necessary to obtain slopes of area distribution for 180° of roll of the configuration with respect to the Mach cone. The five roll angles for the computations used corresponded to angles of 0°, 45°, 90°, 135°, and 180° at a free-stream Mach number of 1.35. All the area distributions and their slopes were determined graphically. The Fourier sine series used for calculating the pressure drags were evaluated for 33 harmonics and plots of these series indicated that they were convergent.

RESULTS AND DISCUSSION

The models used in the present investigation were flight tested through a Mach number range of 0.75 to 1.35. The corresponding Reynolds number (per foot) range was from 4.5×10^6 to 9.5×10^6 as shown in figure 6. The resultant variation of total drag and pressure drag coefficients with Mach number is given in figures 7 to 18.

Effect of Canopy Location

The effects of canopy location on the total drag coefficient for the flat-windshield canopy of fineness ratio 7.00 mounted on the nonindented and indented bodies are presented in figures 7(a) and 7(b), respectively. The curves of total drag coefficient for models A, B, and C (nonindented bodies) show that moving the canopy rearward increased the total drag level of the canopy-fuselage configuration for the transonic and supersonic speed range.

Figure 7(b) shows the variation of total drag coefficient with canopy location for the indented models D, E, and F and shows that the forward canopy location (model D) had the lowest supersonic drag coefficient but that the model with the highest drag coefficient was model E (canopy with $x/l = 0.50$). Since these three models were indented to give the same total cross-sectional area distribution as the basic body alone, the variation of total drag coefficients near $M_\infty = 1.00$ for the three models must be attributed to the accuracy of the data and to local interference effects. However, the variation of the total drag coefficient at $M_\infty = 1.00$ for the three indented bodies was within 10 percent of the total drag coefficient for the basic body alone.

The effects of the canopy location on the pressure drag coefficient are presented in figures 8(a) and 8(b) for the nonindented and indented models, respectively. Figure 8(a) presents the drag rise for the flat-windshield canopies on the nonindented fuselage; also presented in figure 8(a) are the theoretical drag coefficients predicted by the supersonic-area-rule theory. From a comparison of the theoretical and experimental curves in figure 8(a), it is noted that there is an overall relative consistency in the level of predicted wave drag coefficients and the experimental results; hence it seems feasible to use the area-rule theory to predict the pressure drag coefficients expected from a configuration modification. In figure 4 moving the canopies rearward increased the maximum cross-sectional area of the configurations and appears to increase the rate of change of the total cross-sectional area distribution in the vicinity of the canopy. These changes correspond to the increase in drag as the canopy is moved rearward.

The drag-rise coefficients for the indented fuselage models are presented in figure 8(b). The results show that ΔC_D increases as the canopies are moved rearward for transonic and low supersonic speeds, although this was not exactly the case in the total drags shown in figure 7(b).

Effect of Area-Rule Indentation

Figures 9 to 13 present the effect of area-rule indentation on the total drag and the pressure drag coefficients for each canopy tested. Also presented are the curves for the basic body alone in order to provide a convenient method of comparing the effects of the area-rule indentation. In general, the area-rule indentation served to reduce the total drag and the pressure drag at the transonic and low supersonic speeds for all the models investigated. The results also show that the effectiveness of the area-rule indentation decreased as the flight Mach number increased. Figure 14 is included to present a summary plot of all the indented models tested during this investigation. Since all the indented models had the same area distribution and volume, the differences in drag rise shown near $M = 1.0$ are due to both local interference and experimental error.

Effect of Canopy Fineness Ratio

The curves of figures 15 and 16 present the variation of total and pressure drag coefficients for the flat-windshield canopies of fineness ratio 7.00 and 4.50 mounted on the nonindented and indented parabolic bodies.

The curves of figure 15 show that for a nonindented model the short canopy has higher total and pressure drags than the long canopy. The theoretical calculation of pressure drag predicted that the short canopy would have a high pressure drag coefficient and the experimental results verified the prediction.

Figure 16 shows the effect of indenting the fuselage for the short canopy and it appears that the total and pressure drags of the short canopy are still noticeably higher than those of the indented model with the long canopy.

Effect of Windshield Shape

Figure 17 presents the variation of total and pressure drag coefficients for the flat- and vee-windshield canopies of fineness ratio 7.00 mounted on the nonindented fuselage. The curves show that there was relatively little difference in total drag between the two windshield shapes investigated. The theoretical calculations of pressure drag predicted also that the vee windshield would have slightly higher pressure drag than the flat windshield.

Figure 18 presents the results for the two windshield shapes mounted on indented fuselages. The results indicate a negligible variation in

total and pressure drags at the transonic and low supersonic speeds and there appears to be an increasing difference in total and pressure drags for the two windshields as the flight velocity increases.

CONCLUDING REMARKS

The present investigation was conducted to determine the total drag and pressure drag coefficients of several canopy-fuselage combinations and to determine the effect on the drag coefficient of canopy location along the basic parabolic fuselage, windshield shape, canopy fineness ratio, and area-rule indentation. The flight tests were conducted with free-flight models flown through a Mach number range of 0.75 to 1.35. The data included comparison of experimental results with the theoretical pressure drag coefficients which were computed for some of the models tested by using the supersonic-area-rule theory.

The tests of the canopies on the parabolic fuselage showed that the total drag and pressure drag increased as the canopy location was moved rearward to the maximum body diameter station. There was a negligible difference in drag due to windshield shape. The effect of fineness ratio was to increase the drag when the canopy fineness ratio was decreased.

Indenting the fuselage for a Mach number of 1.00 lowered the total drag and pressure drag coefficients at the transonic and low supersonic speeds for all the canopies tested. The effectiveness of the indentation decreased with increasing Mach number. Comparison of the model pressure drag determined by the area-rule theory with the experimental results indicated favorable correlation in the ability of the area-rule theory to predict pressure drag variations with canopy configuration modifications. Since the five indented models tested had the same total cross-sectional area and volume distributions, the differences in drag obtained at transonic and low supersonic speeds, for these models, were due to both local interference effects and experimental error.

Langley Aeronautical Laboratory,
National Advisory Committee for Aeronautics,
Langley Field, Va., September 2, 1958.

REFERENCES

1. Welch, Clement J., and Morrow, John D.: Flight Investigation at Mach Numbers From 0.8 to 1.5 of the Drag of a Canopy Located at Two Positions on a Parabolic Body of Revolution. NACA RM L51A29, 1951.

2. Cornette, Eldon S., and Robinson, Harold L.: Transonic Wind-Tunnel Investigation of Effects of Windshield Shape and Canopy Location on the Aerodynamic Characteristics of Canopy-Body Combinations. NACA RM L55G08, 1955.

3. Van Driest, E. R.: Turbulent Boundary Layer in Compressible Fluids. Jour. Aero. Sci., vol. 18, no. 3, Mar. 1951, pp. 145-160, 216.

4. Morrow, John D., and Nelson, R. L.: Large-Scale Flight Measurements of Zero-Lift Drag of 10 Wing-Body Configurations at Mach Numbers From 0.8 to 1.6. NACA RM L52D18a, 1953.

5. Jones, Robert T.: Theory of Wing-Body Drag at Supersonic Speeds. NACA Rep. 1284, 1956.

6. Holdaway, George H.: Comparison of Theoretical and Experimental Zero-Lift Drag-Rise Characteristics of Wing-Body-Tail Combinations Near the Speed of Sound. NACA RM A53H17, 1953.

7. Alksne, Alberta: A Comparison of Two Methods for Computing the Wave Drag of Wing-Body Combinations. NACA RM A55A06a, 1955.

TABLE I

DESCRIPTION OF MODELS

Model	Windshield shape	Canopy fineness ratio		Canopy location, x/l	Fuselage
		Nominal	Actual		
A	Flat	7.00	7.00	0.30	Nonindented
B	Flat	7.00	7.07	.50	Nonindented
C	Flat	7.00	6.93	.75	Nonindented
D	Flat	7.00	6.05	.30	Indented
E	Flat	7.00	6.35	.50	Indented
F	Flat	7.00	6.35	.75	Indented
G	Flat	4.50	4.55	.50	Nonindented
H	Flat	4.50	4.10	.50	Indented
I	Vee	7.00	7.57	.45	Nonindented
J	Vee	7.00	6.81	.45	Indented

TABLE II

FUSELAGE COORDINATES

[Station measured from leading point of fuselage]

(a) Basic parabolic body and models A, B, C, G, and I

x, in.	y_r, in.
0	0
2.0	.475
4.0	.900
5.0	1.094
6.0	1.275
8.0	1.600
10.0	1.875
12.0	2.100
14.0	2.275
16.0	2.400
18.0	2.475
20.0	2.500
22.0	2.495
24.0	2.478
26.0	2.450
28.0	2.412
30.0	2.361
32.0	2.300
34.0	2.225
36.0	2.145
38.0	2.050
40.0	1.945
42.0	1.828
44.0	1.700
46.0	1.561
48.0	1.411
50.0	1.250

(b) Model D

x, in. (1)	y_r, in. (1)
5	1.094
6	1.275
7	1.386
8	1.377
9	1.350
10	1.488
11	1.701
12	1.874
13	2.034
14	2.157
15	2.265
16	2.349
17	2.415
18	2.473
19	2.494
20	2.500

[1]Coordinates before station 5 and after station 20 are the same as the basic body coordinates.

(c) Model E

x, in. (1)	y_r, in. (1)
5	1.094
6	1.275
8	1.600
10	1.875
11	1.948
12	1.957
13	1.930
14	1.992
15	2.098
16	2.198
17	2.287
18	2.358
19	2.408
20	2.443
21	2.459
22	2.476
23	2.482
24	2.478

[1]Coordinates before station 5 and after station 24 are the same as the basic body coordinates.

(d) Model F

x, in. (1)	y_r, in. (1)
14	2.275
15	2.344
16	2.362
17	2.327
18	2.249
19	2.238
20	2.254
21	2.282
22	2.316
23	2.349
24	2.378
25	2.394
26	2.407
27	2.409
28	2.404
29	2.388
30	2.361

[1]Coordinates before station 14 and after station 30 are the same as the basic body coordinates.

(e) Model H

x, in. (1)	y_r, in. (1)
5	1.095
6	1.275
8	1.600
10	1.875
11	1.946
12	1.955
13	1.932
14	1.992
15	2.122
16	2.256
17	2.369
18	2.450
20	2.500

[1]Coordinates before station 5 and after station 20 are the same as the basic body coordinates.

(f) Model J

x, in. (1)	y_r, in. (1)
5	1.094
6	1.275
8	1.600
9	1.744
10	1.857
11	1.915
12	1.926
13	1.921
14	1.997
15	2.098
16	2.198
17	2.287
18	2.358
19	2.408
20	2.443
21	2.459
22	2.476
23	2.482
24	2.478

[1]Coordinates before station 5 and after station 24 are the same as the basic body coordinates.

TABLE III

CANOPY COORDINATES

[Station measured from canopy leading edge]

(a) Models A to F

Station, in.	y_c, in.	r_c, in.
0	2.250	0.625
1.0	2.200	.825
2.0	2.335	1.125
3.0	2.495	1.350
4.0	2.585	1.395
5.0	2.650	1.350
6.0	2.695	1.275
7.0	2.730	1.175
8.0	2.750	1.060
9.0	2.765	.935
10.0	2.760	.815
11.0	2.750	.695
12.0	2.739	.545
13.0	2.740	.365
14.0	2.765	.163

(b) Models G and H

Station, in.	y_c, in.	r_c, in.
0	2.250	0.625
1	2.200	.825
2	2.335	1.125
3	2.495	1.350
4	2.585	1.395
5	2.680	1.285
6	2.710	1.110
7	2.690	.905
8	2.635	.675
9	2.650	.310

(c) Models I and J

Station, in.	y_c, in.	r_c, in.
0	2.095	0.115
1	2.200	.550
2	2.305	.955
3	2.400	1.215
4	2.505	1.360
5	2.585	1.395
6	2.650	1.350
7	2.695	1.275
8	2.730	1.175
9	2.750	1.060
10	2.765	.935
11	2.760	.815
12	2.750	.695
13	2.735	.545
14	2.740	.365
15	2.765	.163

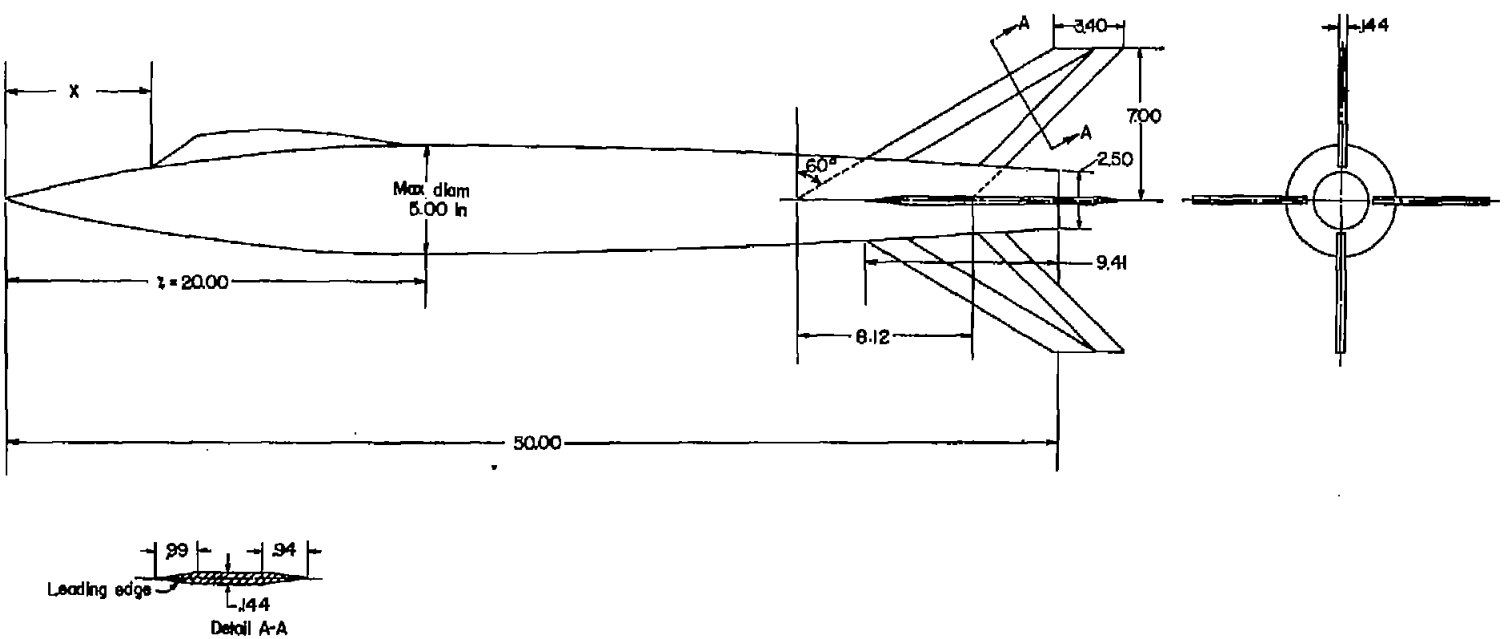

(a) Basic fuselage with a canopy.

Figure 1.- Details and dimensions of models tested. All dimensions are in inches unless otherwise noted.

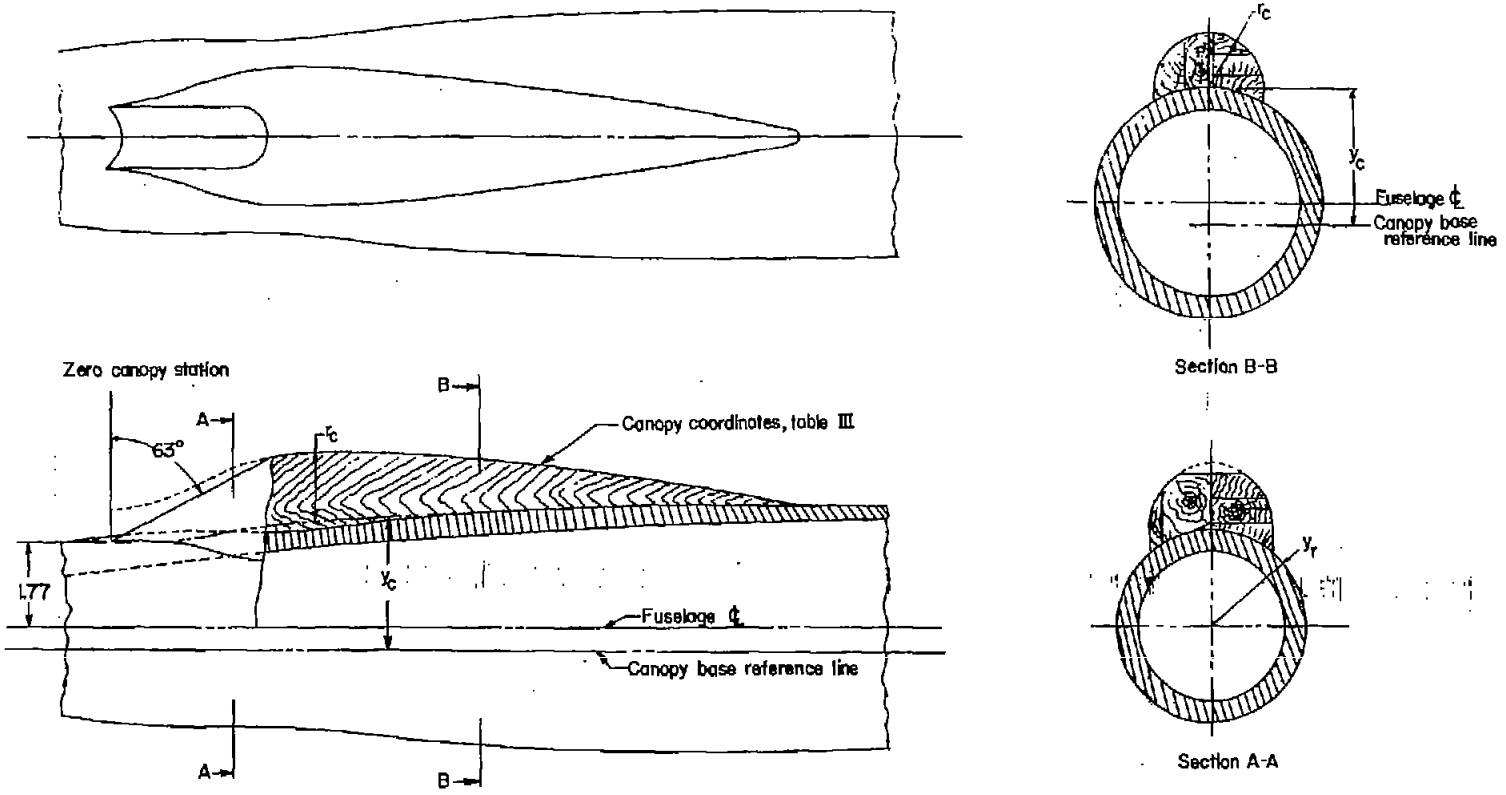

(b) Typical canopy with flat windshield on indented body.

Figure 1.- Continued.

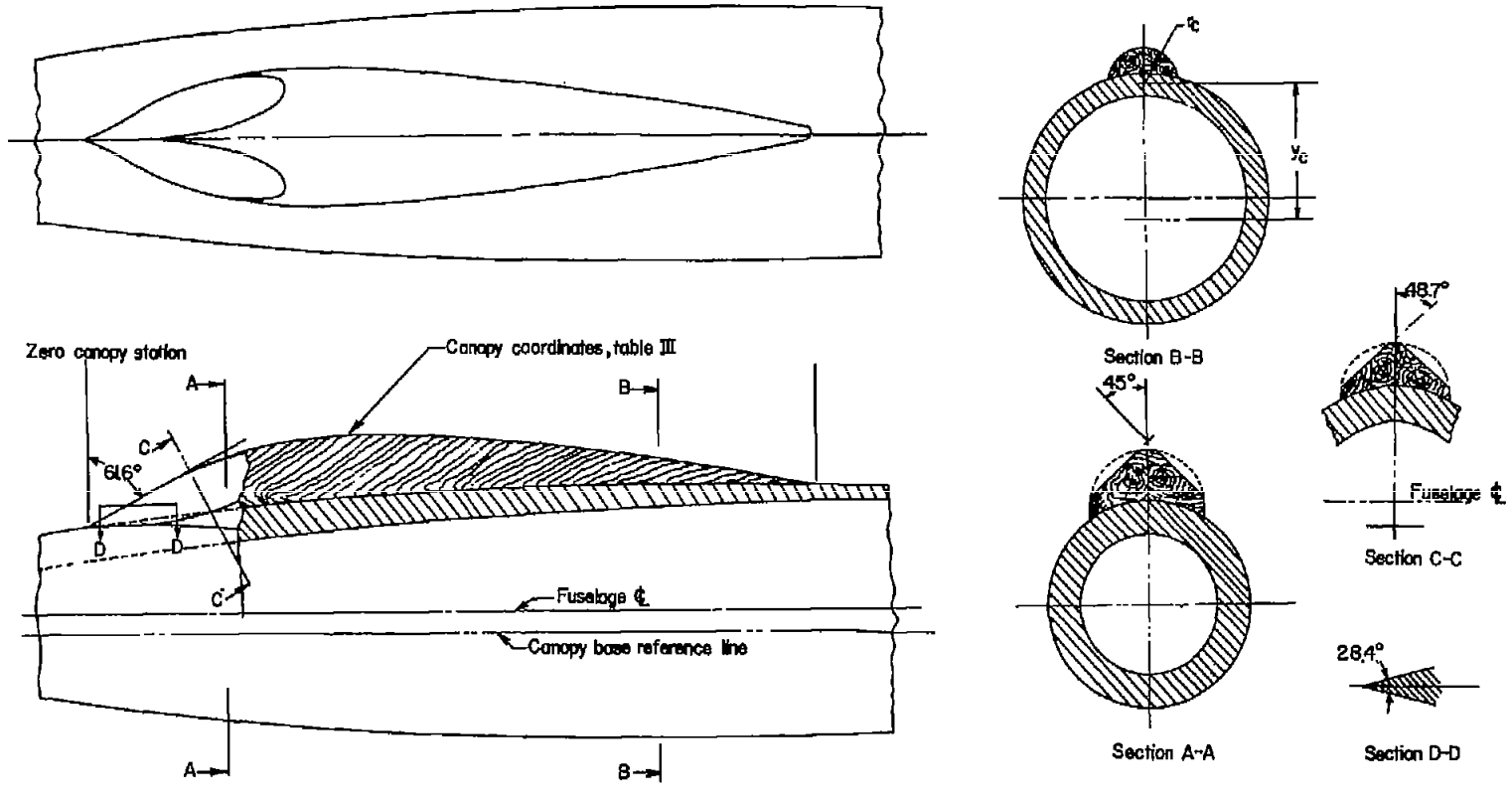

(c) Typical canopy with vee windshield on unindented fuselage.

Figure 1.- Concluded.

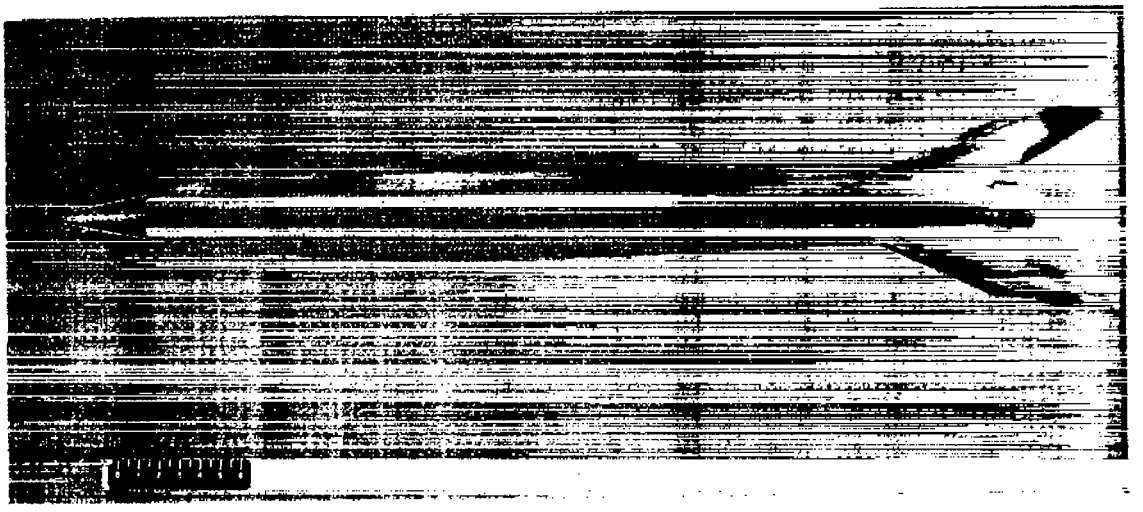

Model A (Nonindented)

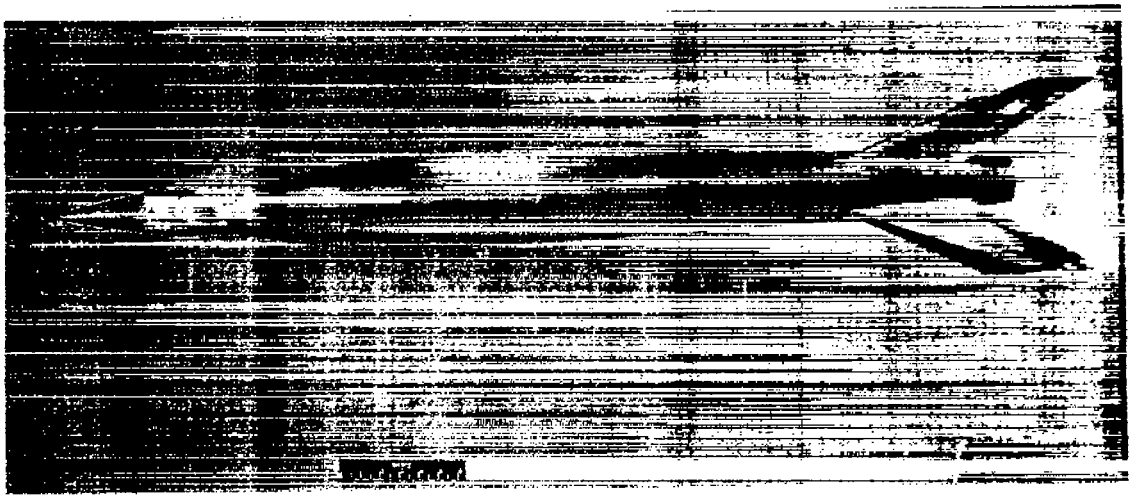

Model D (Indented) L-58-2533

Figure 2.- Typical canopy-fuselage-fin configuration showing nonindented and indented model.

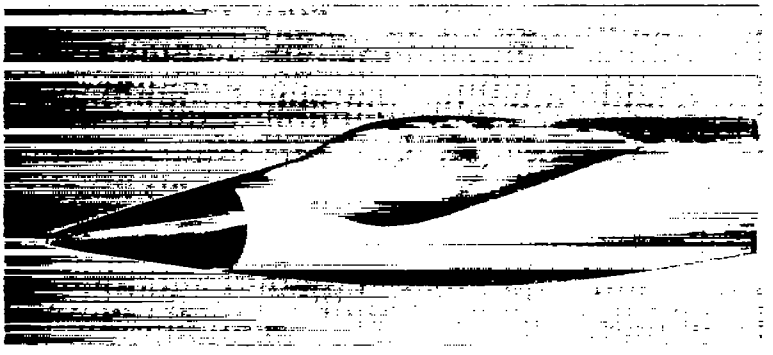

(a) Model A.

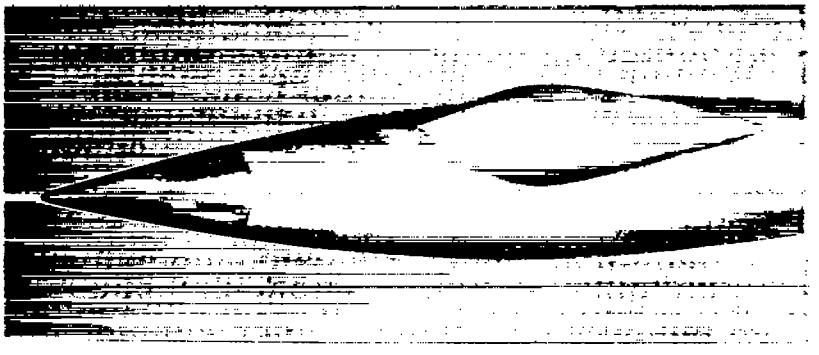

(b) Model B.

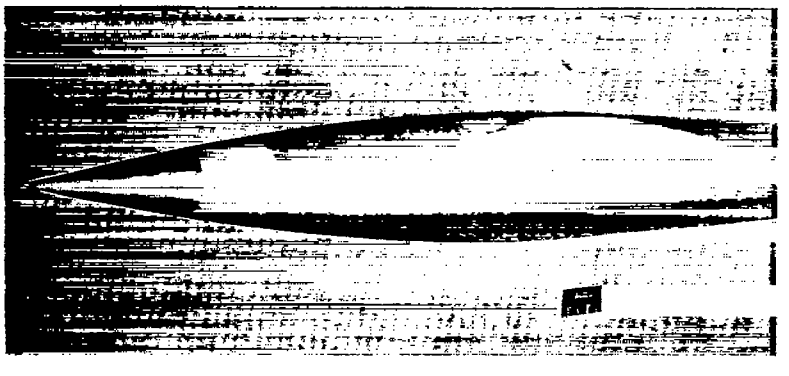

(c) Model C. L-58-2534

Figure 3.- Photographs of the models tested showing the various fuselage-canopy combinations.

(d) Model D.

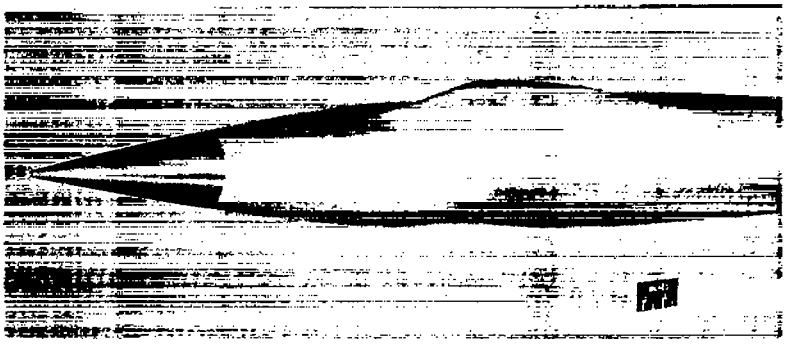

(e) Model E.

(f) Model F. L-58-2535

Figure 3.- Continued.

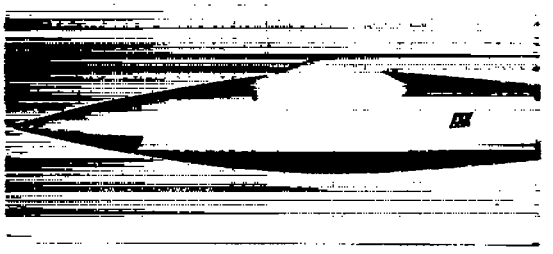

(g) Model G.

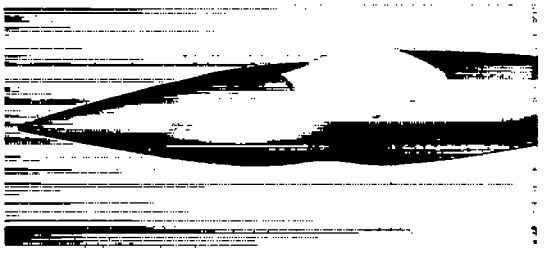

(h) Model H.

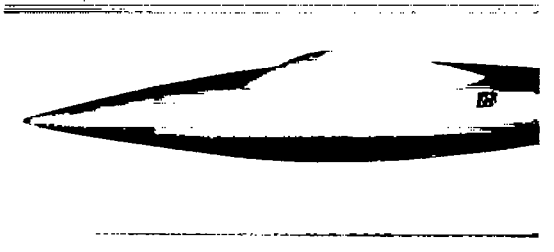

(i) Model I.

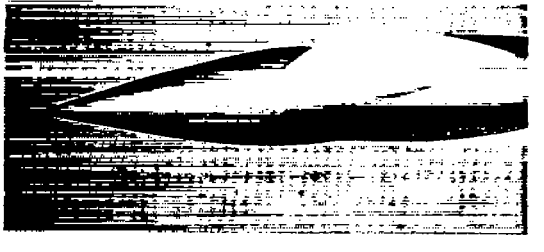

(j) Model J.

L-58-2536

Figure 3.- Concluded.

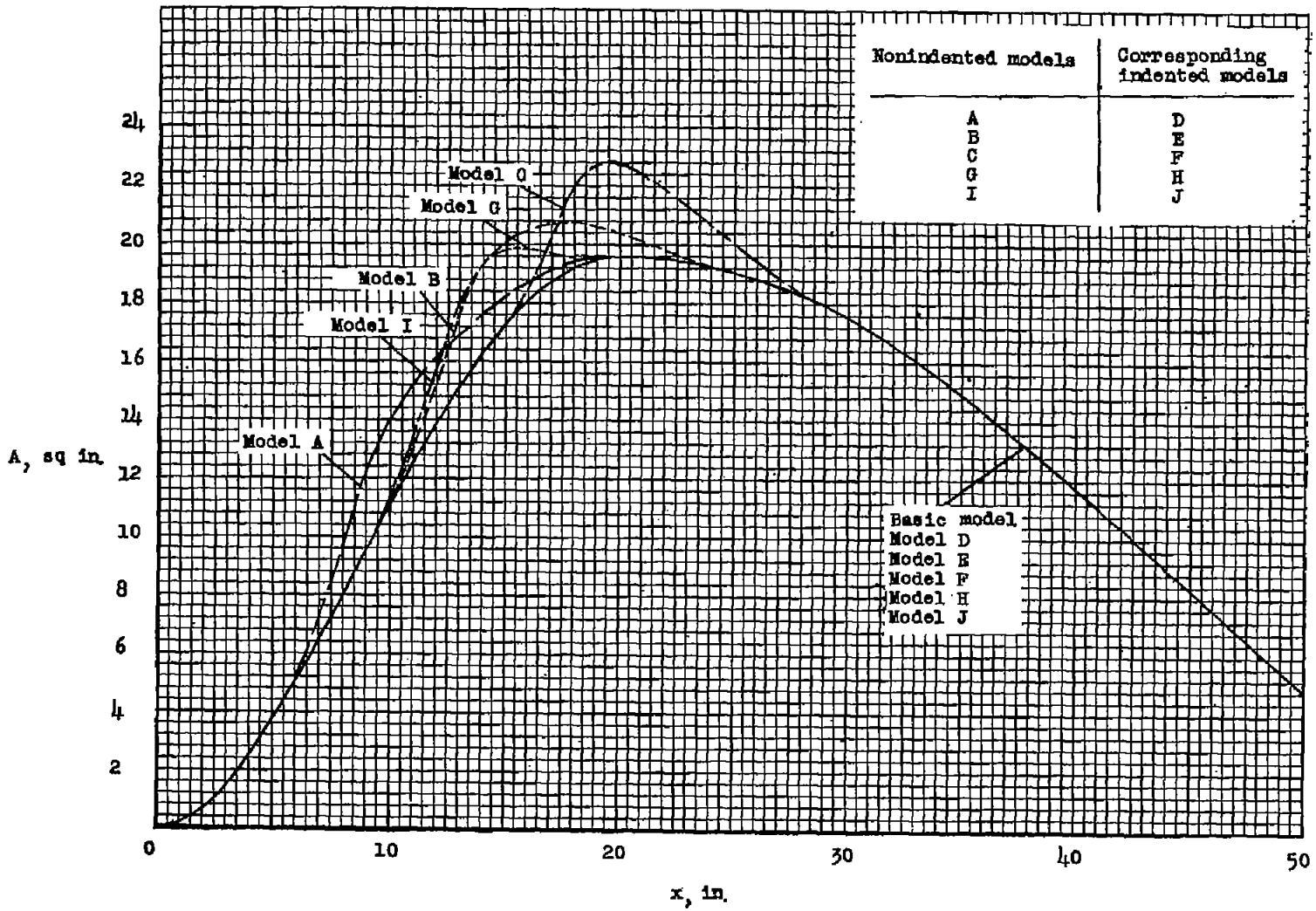

Figure 4.- Variation of the normal cross-sectional area for canopy-fuselage combinations (without fins).

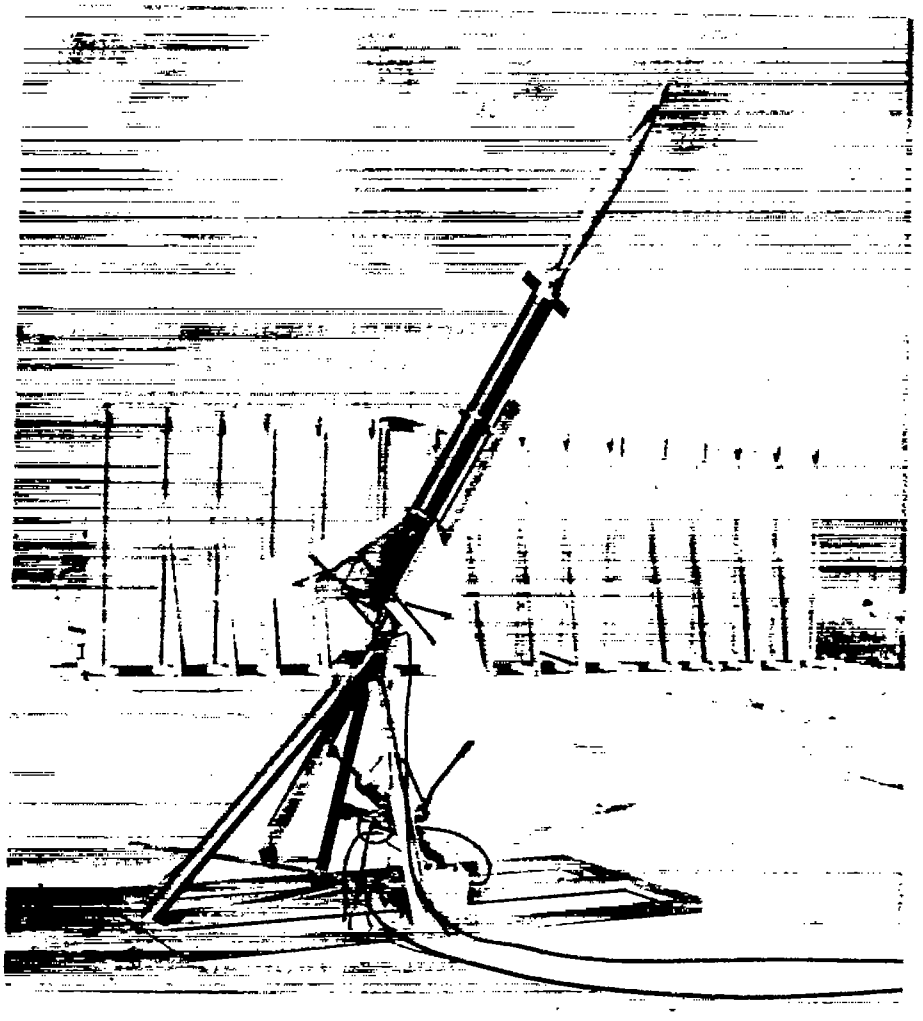

L-94729.1

Figure 5.- Photograph of a typical model and booster arrangement on the launcher prior to launching.

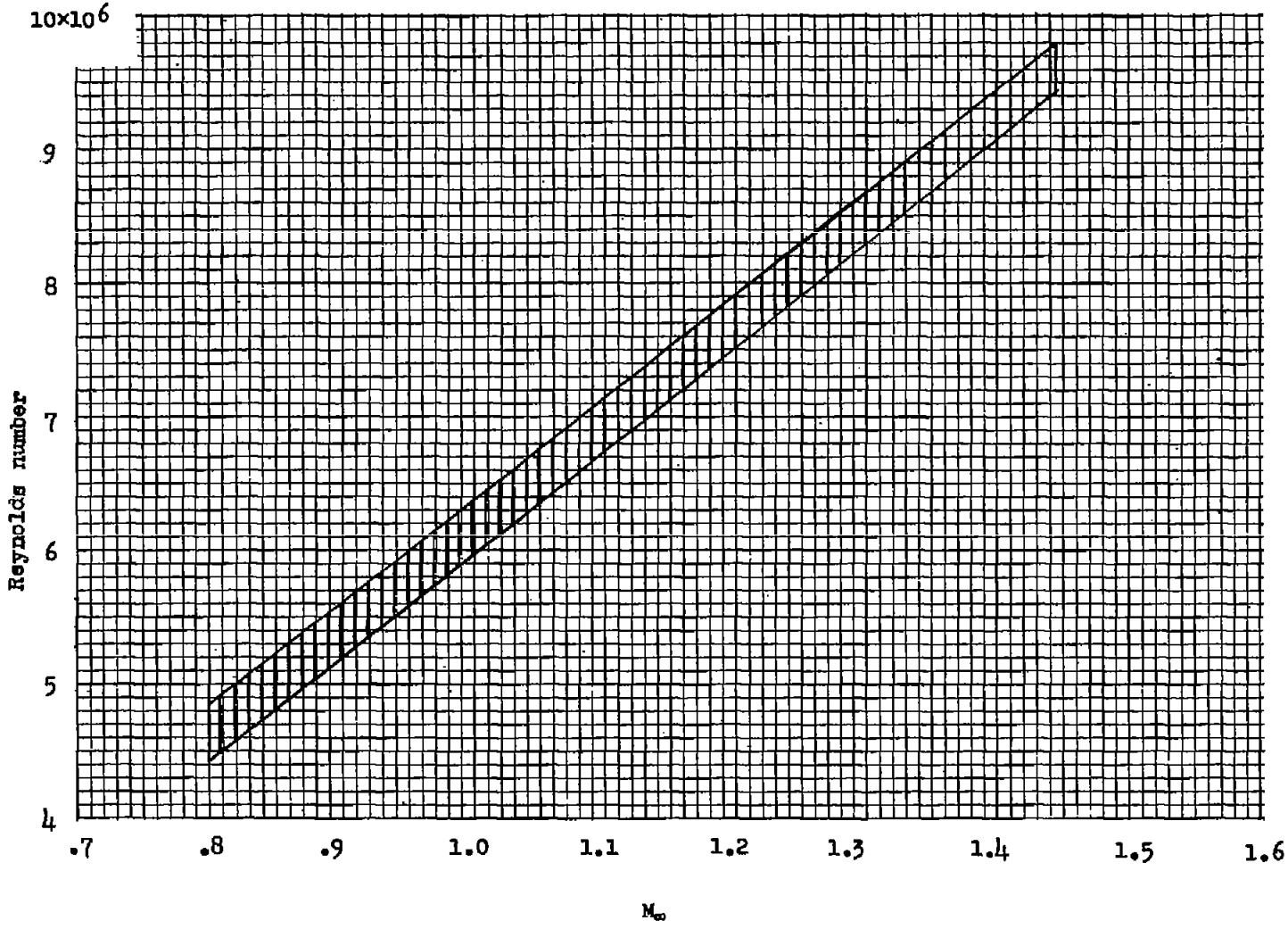

Figure 6.- Variation of Reynolds number with Mach number for models tested. (Reynolds number based on length of 1 foot.)

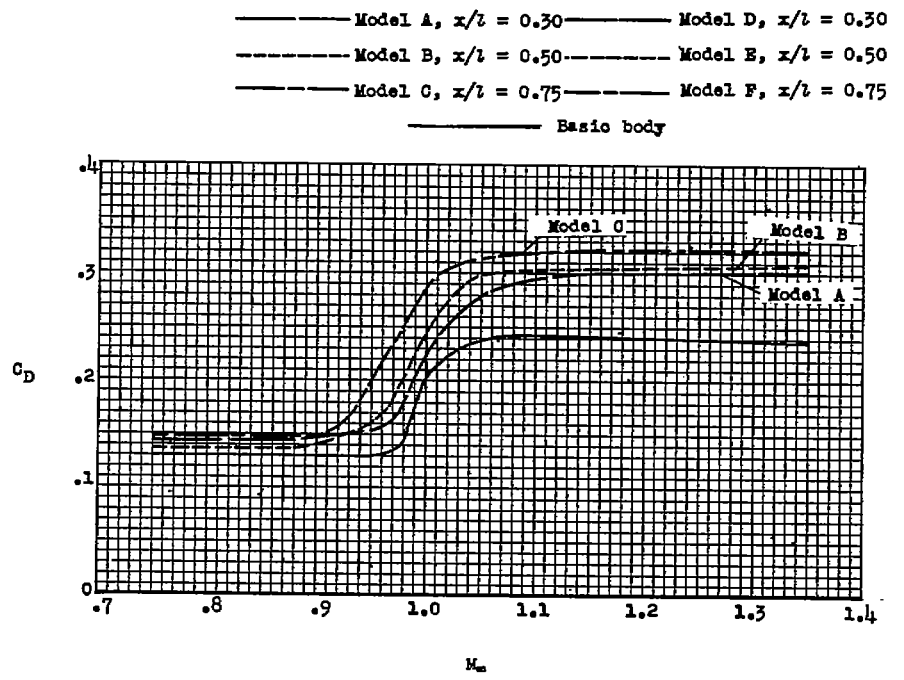

(a) Nonindented models.

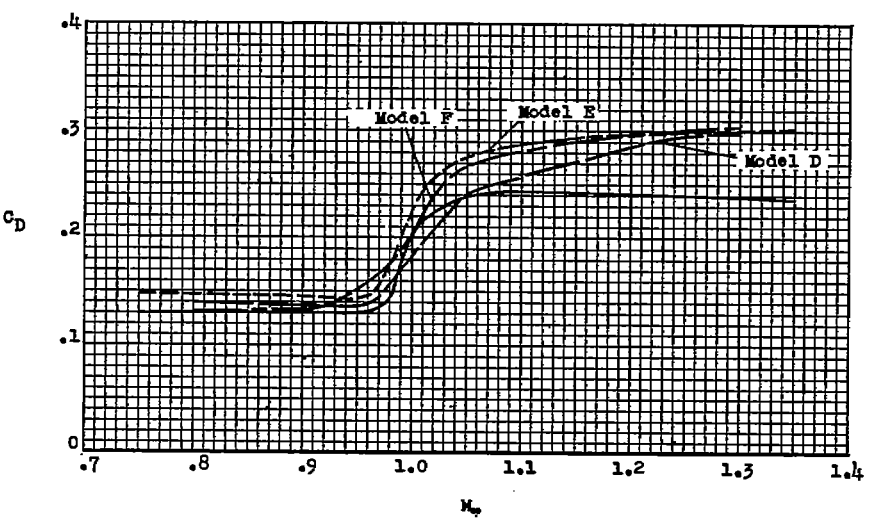

(b) Indented models.

Figure 7.- Variation of total drag coefficient with Mach number for the flat-windshield canopies of fineness ratio 7.00 showing the effect of canopy longitudinal location on drag.

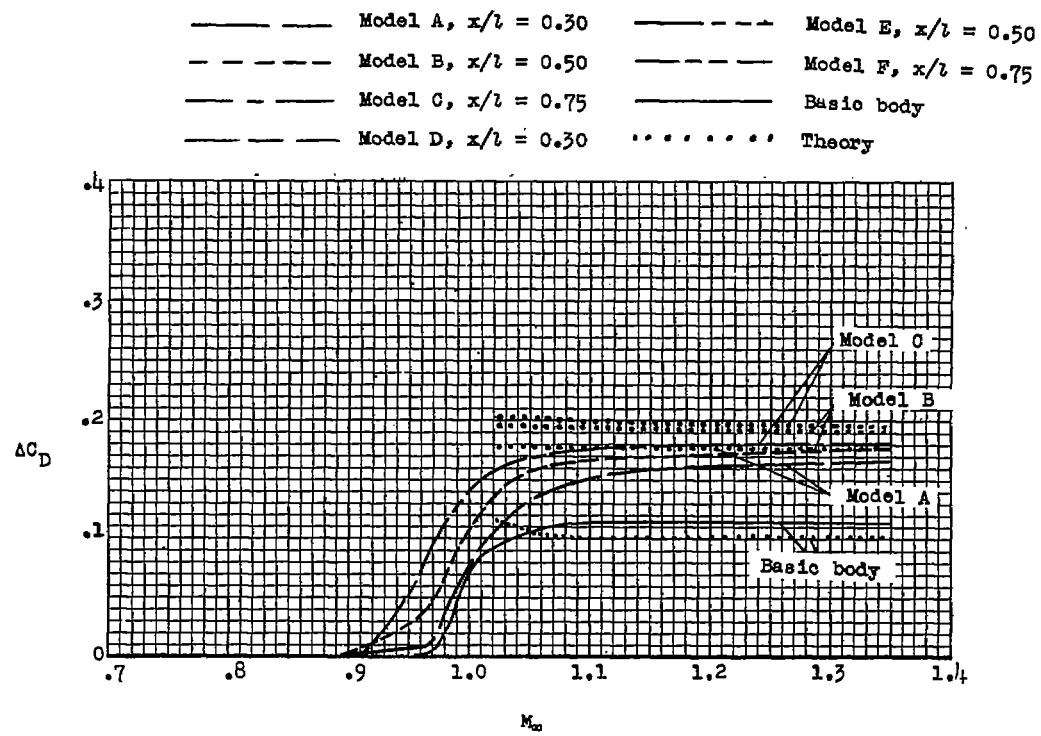

(a) Nonindented models.

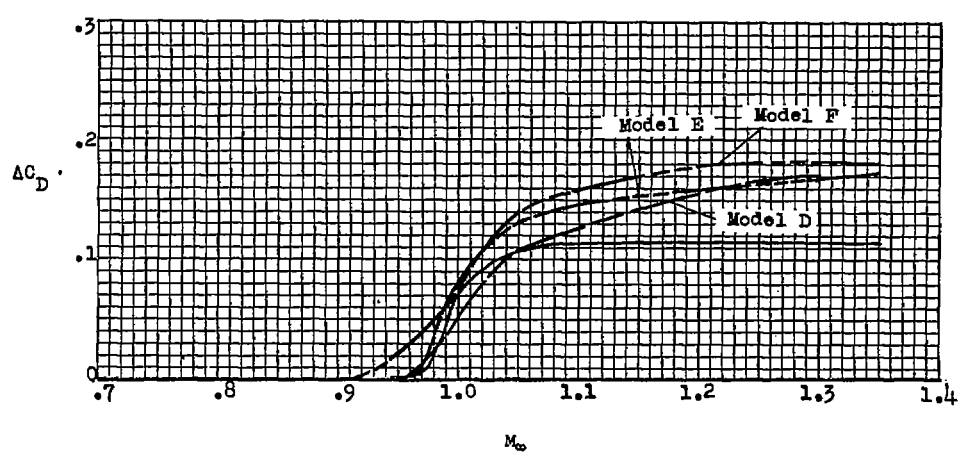

(b) Indented models.

Figure 8.- Variation of pressure drag coefficient with Mach number for the flat-windshield canopy of fineness ratio 7.00 showing the effect of canopy longitudinal location on drag.

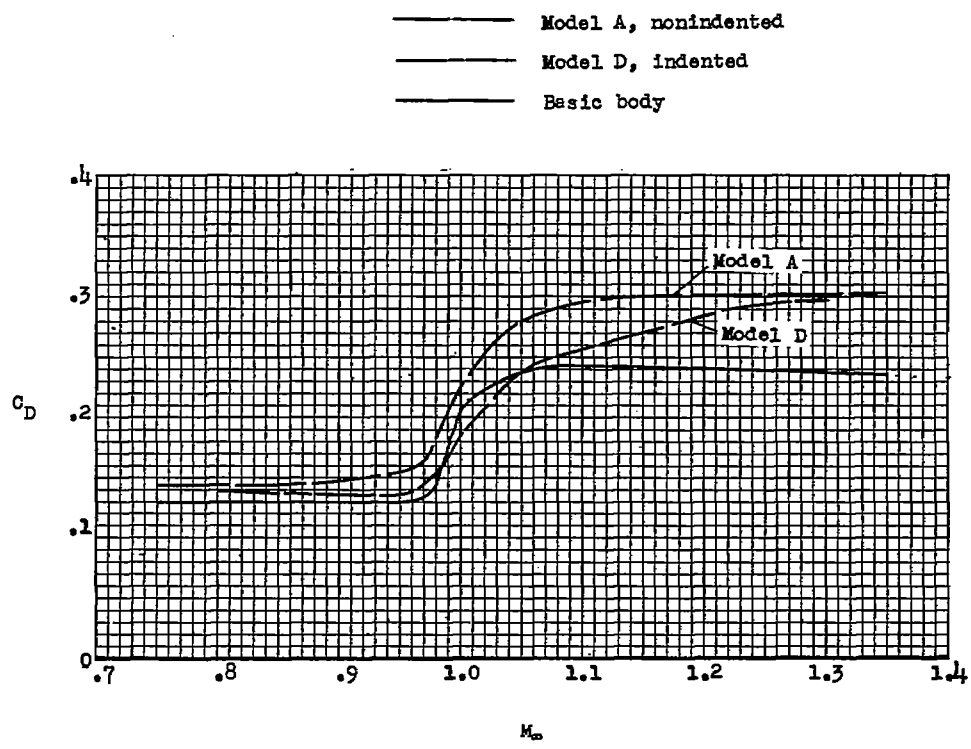

(a) Total drag.

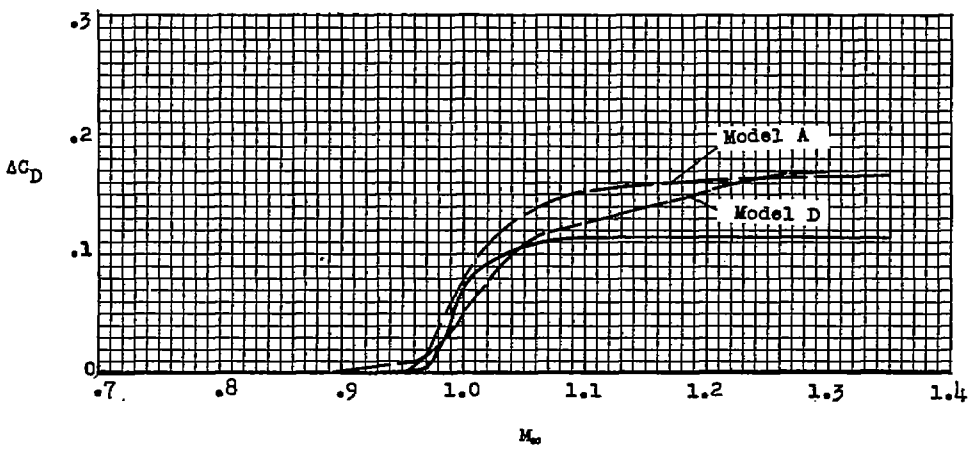

(b) Pressure drag.

Figure 9.- Effect of indentation on total drag and pressure drag for the model with the flat-windshield canopy of fineness ratio 7.00 at the forward position (x/l = 0.30).

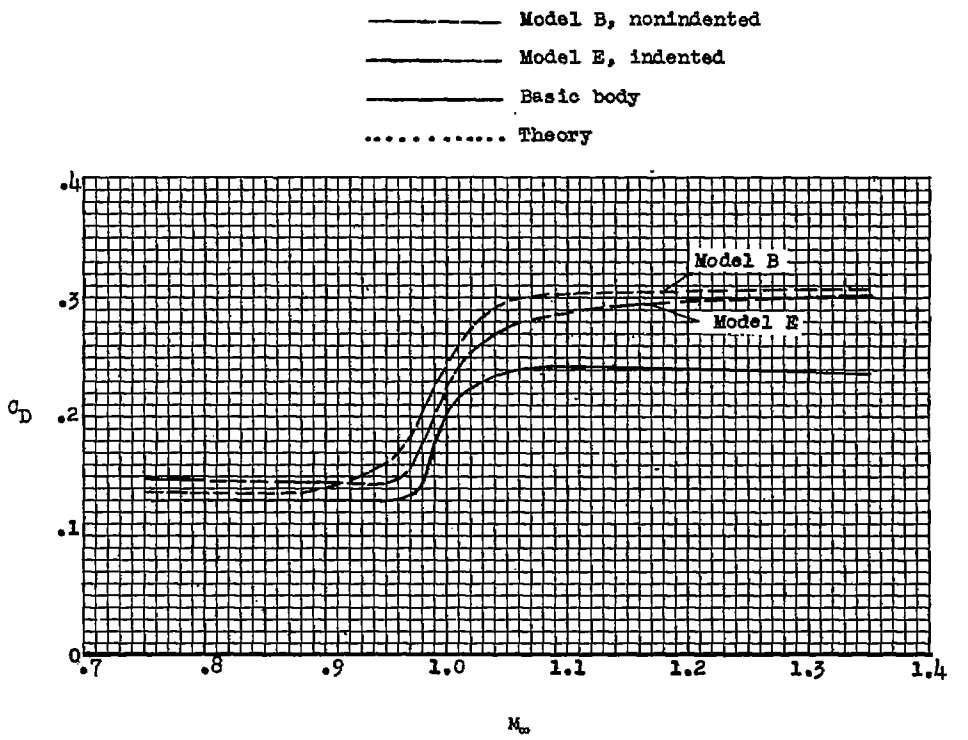

(a) Total drag.

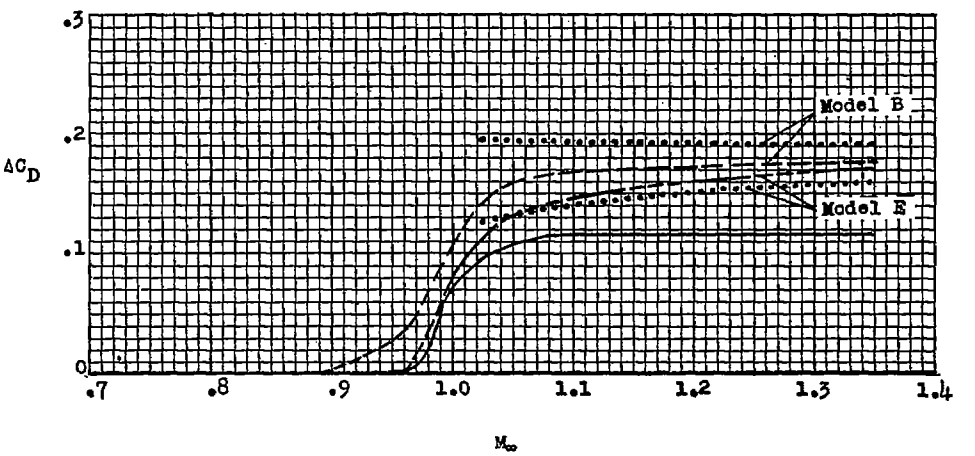

(b) Pressure drag.

Figure 10.- Effect of indentation on total drag and pressure drag for the model with the flat-windshield canopy of fineness ratio 7.00 at the midposition (x/l = 0.50).

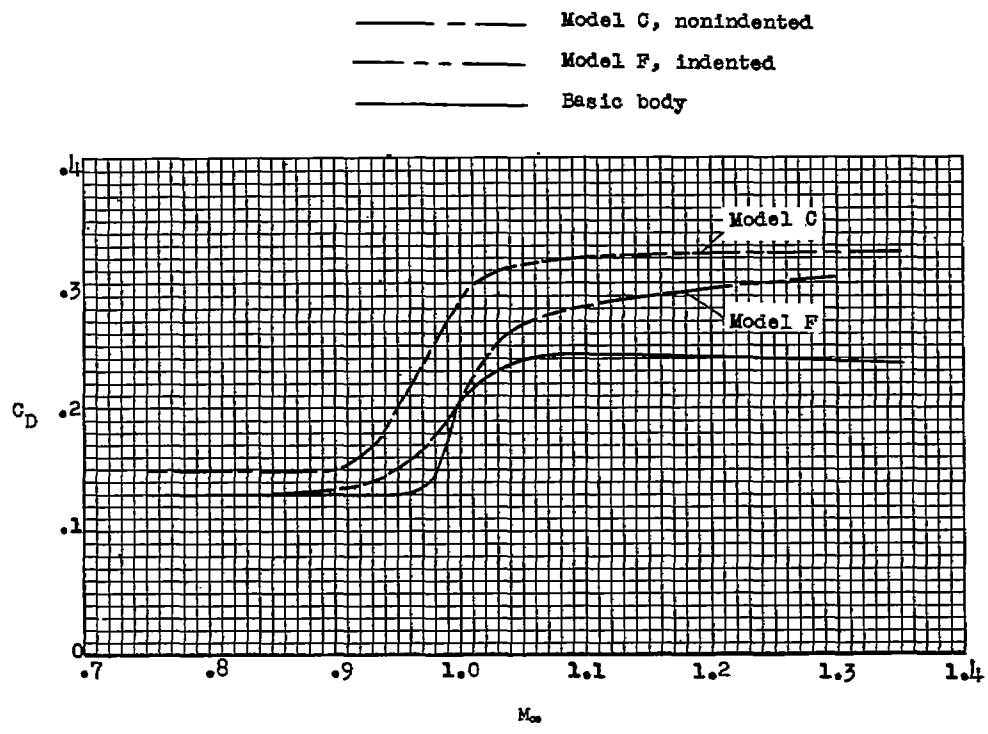

(a) Total drag.

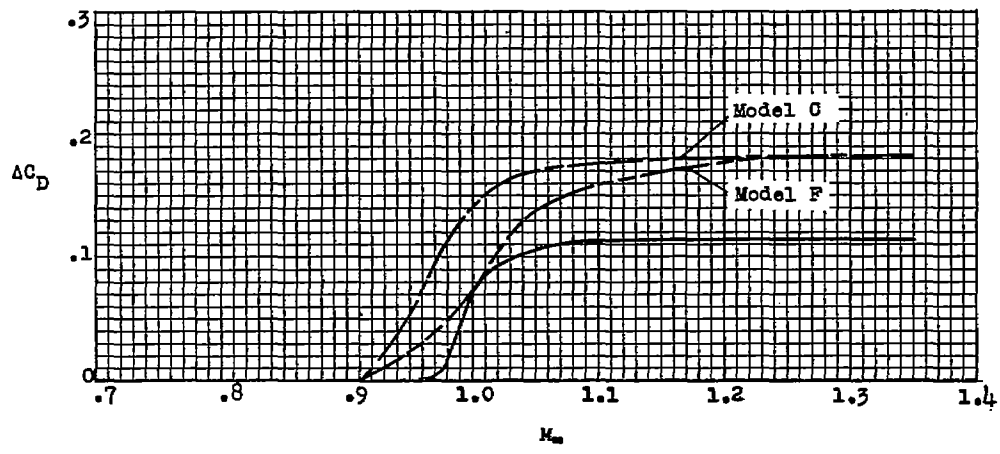

(b) Pressure drag.

Figure 11.- Effect of indentation on total drag and pressure drag for the model with the flat-windshield canopy of fineness ratio 7.00 at the rear position ($x/l = 0.75$).

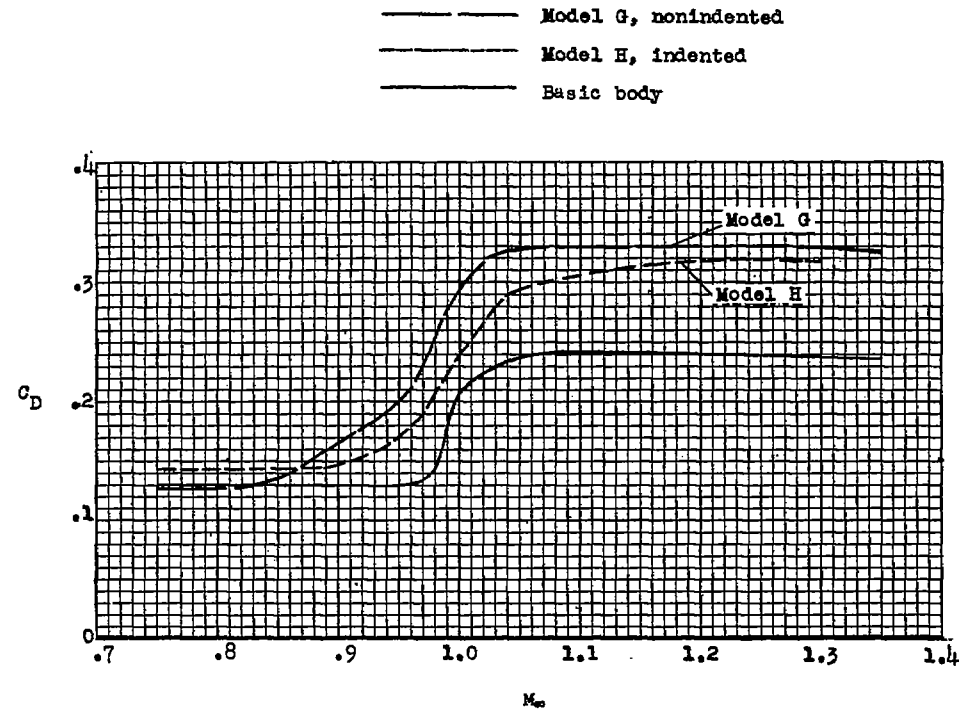

(a) Total drag.

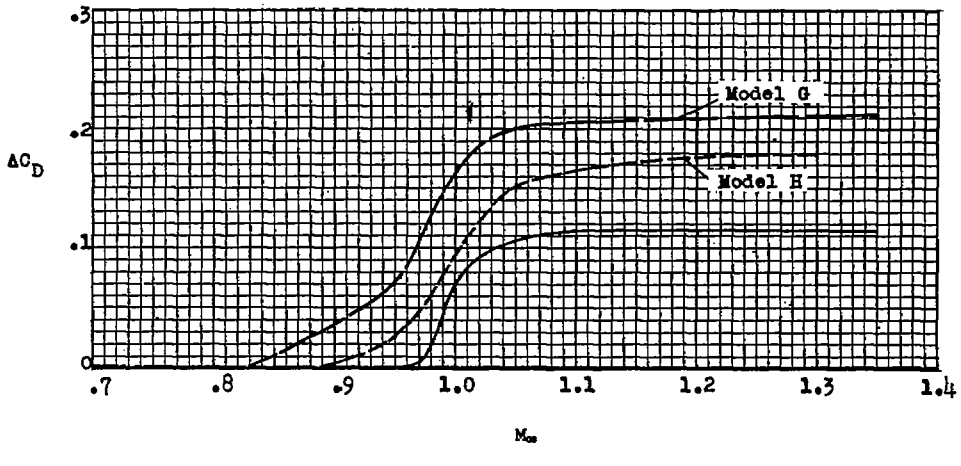

(b) Pressure drag.

Figure 12.- Effect of indentation on total drag and pressure drag for the model with the flat-windshield canopy of fineness ratio 4.50 at the midposition (x/l = 0.50).

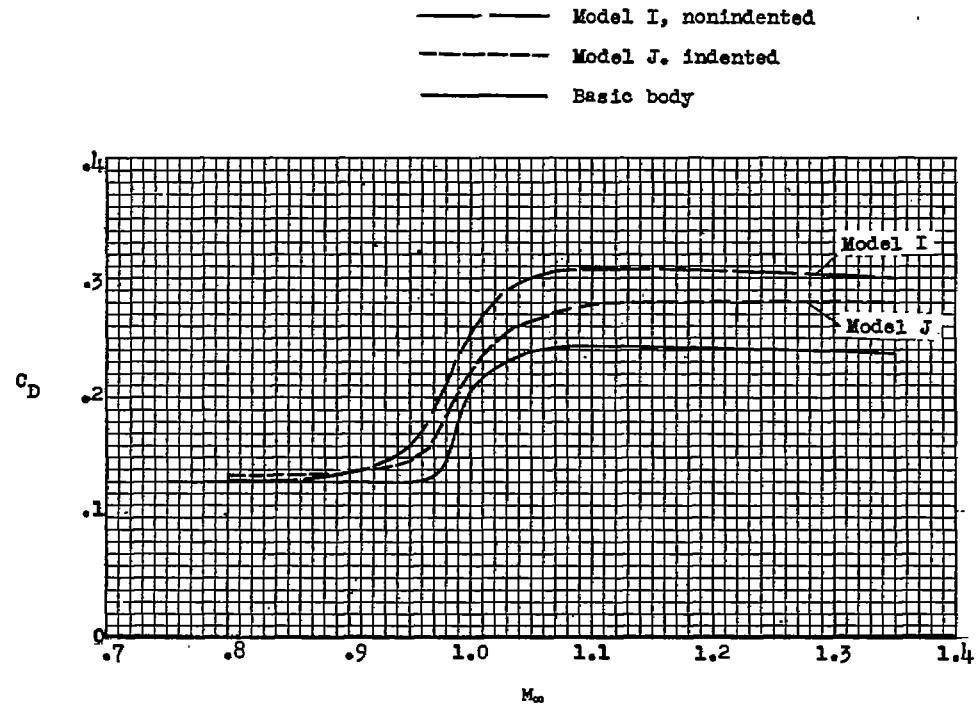

(a) Total drag.

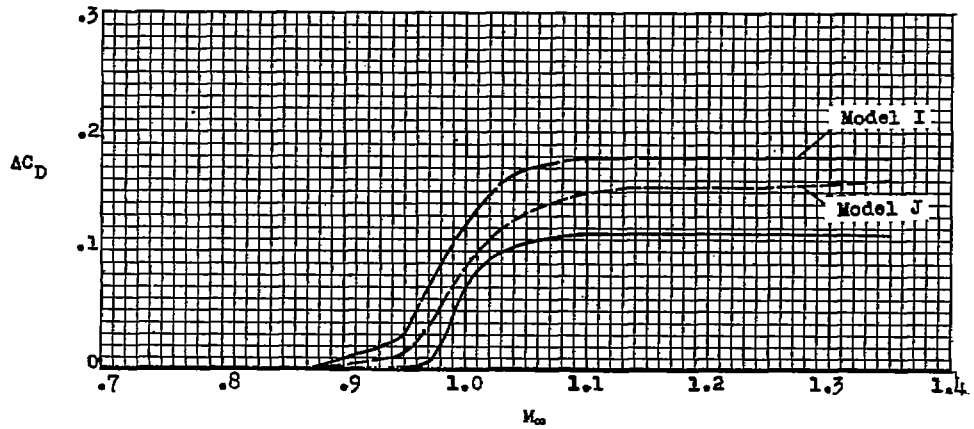

(b) Pressure drag.

Figure 13.- Effect of indentation on total drag and pressure drag for the model with the vee-windshield canopy of fineness ratio 7.00 at the midposition ($x/l = 0.50$).

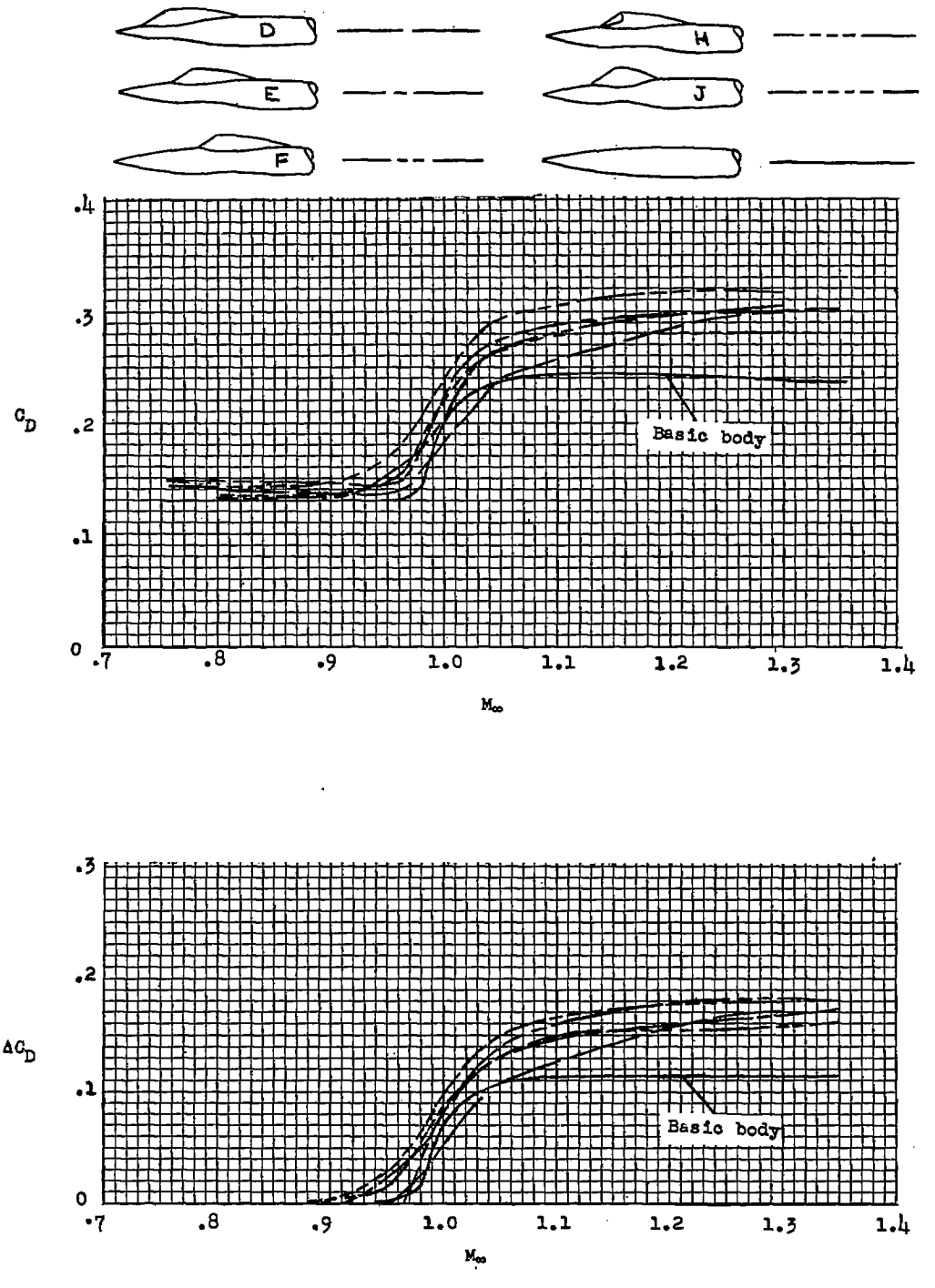

Figure 14.- Summary of total drag coefficients and pressure drag coefficients for all area-rule-indented models investigated.

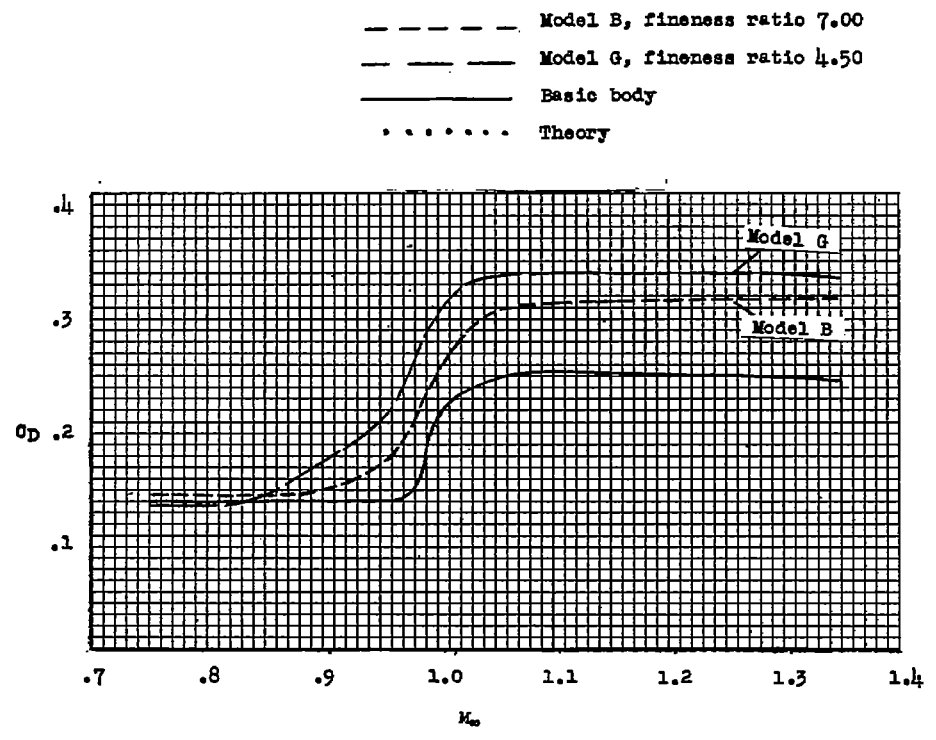

(a) Total drag.

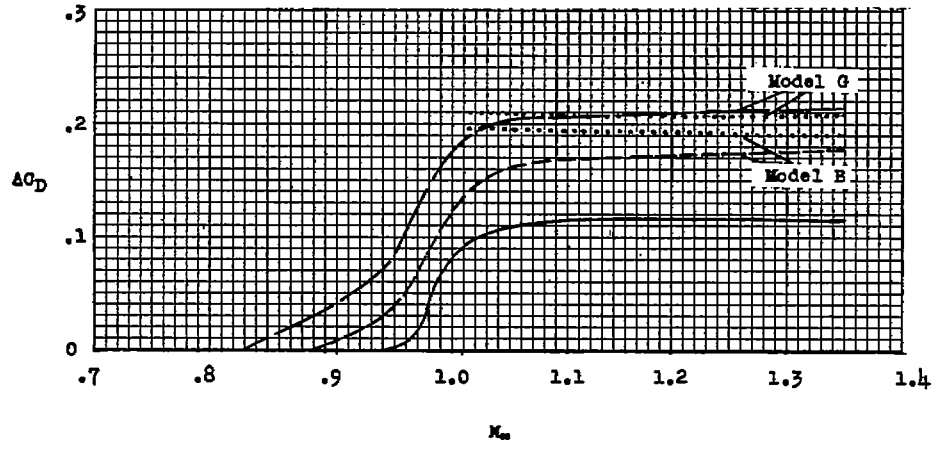

(b) Pressure drag.

Figure 15.- Comparison of total drag and pressure drag coefficients of models with flat-windshield canopies of fineness ratio 7.00 and 4.50 at the midposition ($x/l = 0.50$) on the nonindented fuselage.

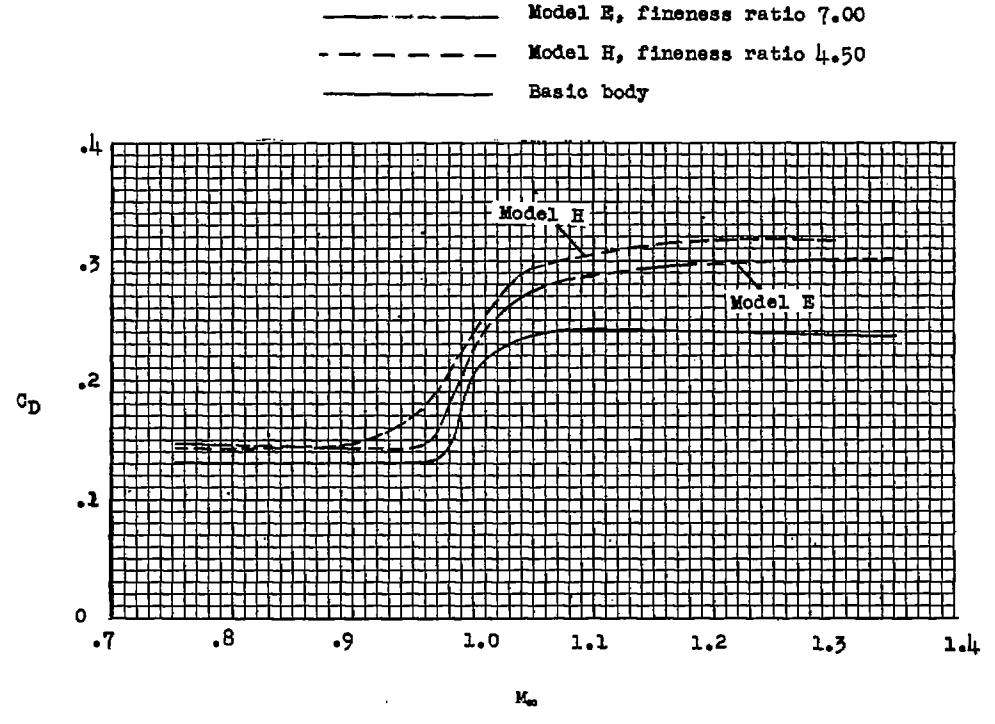

(a) Total drag.

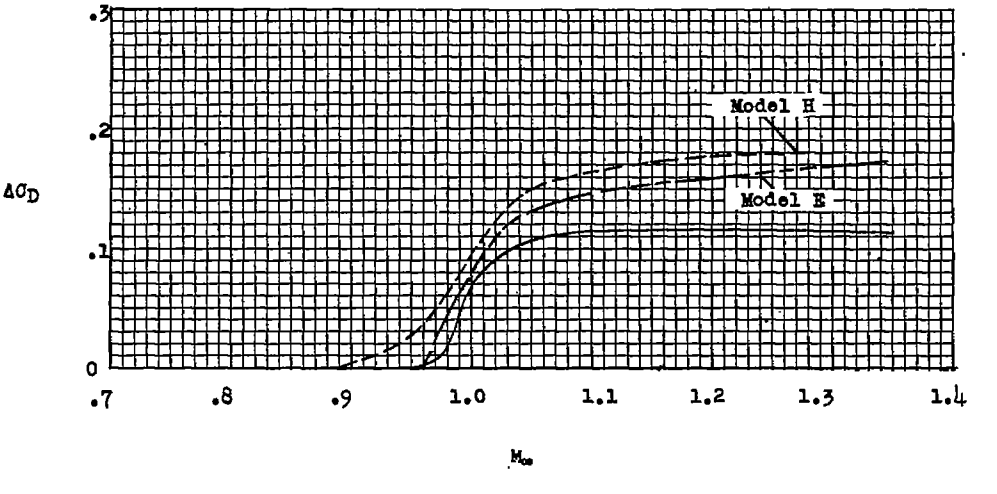

(b) Pressure drag.

Figure 16.- Comparison of total drag and pressure drag coefficients of models with flat-windshield canopies of fineness ratio 7.00 and 4.50 at the midposition (x/l = 0.50) on the indented fuselage.

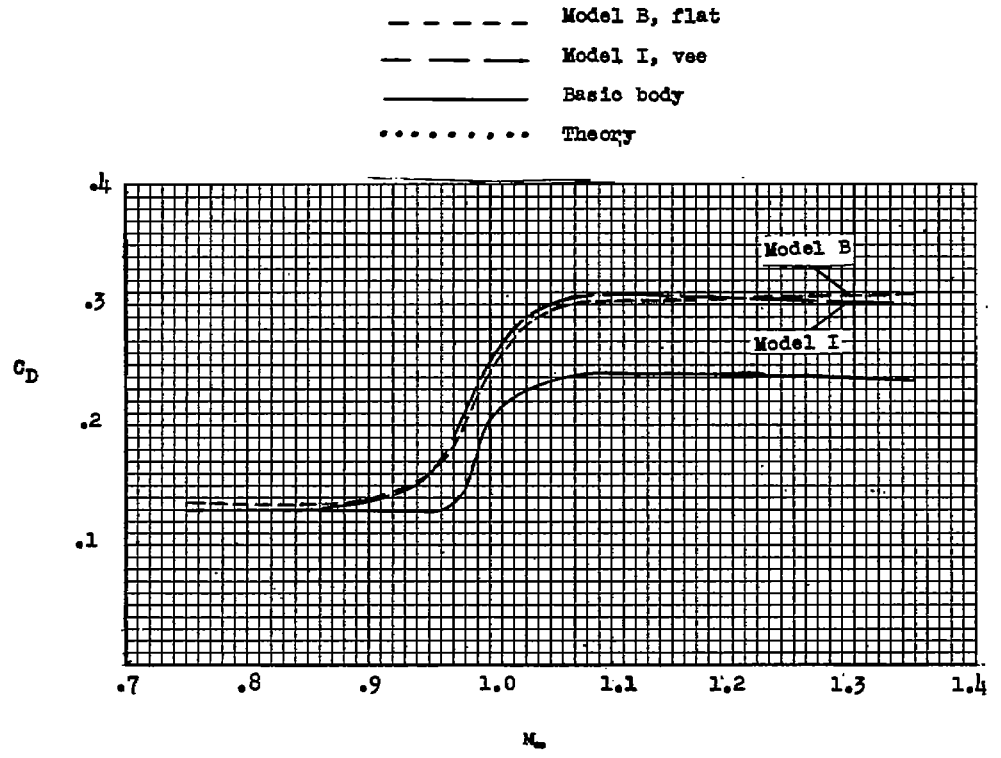

(a) Total drag.

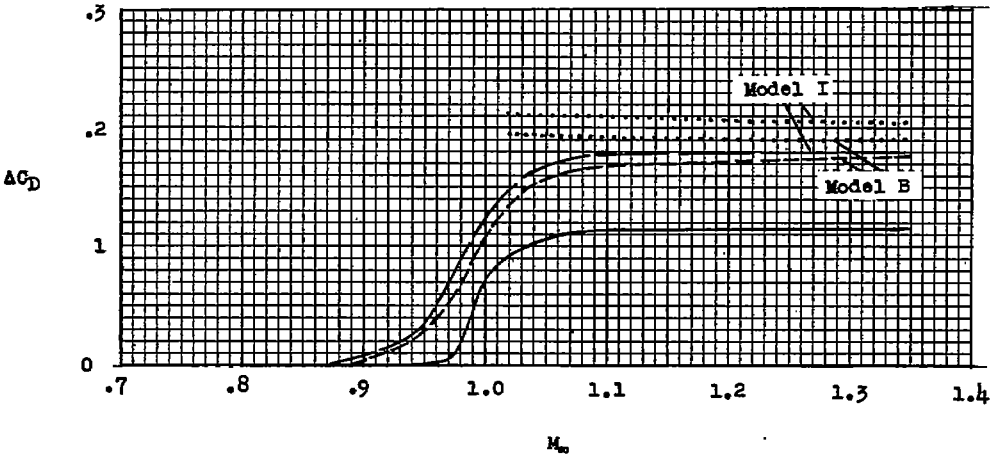

(b) Pressure drag.

Figure 17.- Comparison of total drag and pressure drag coefficients of fineness-ratio-7.00 canopies with flat and vee windshields at mid-position (x/l = 0.50) on the nonindented fuselage.

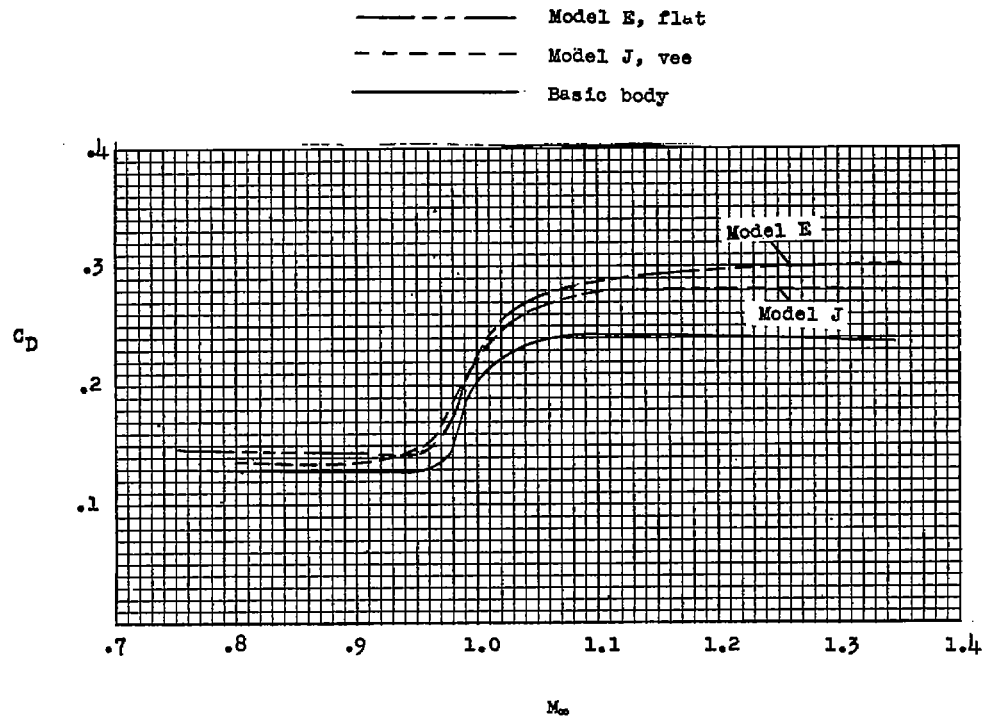

(a) Total drag.

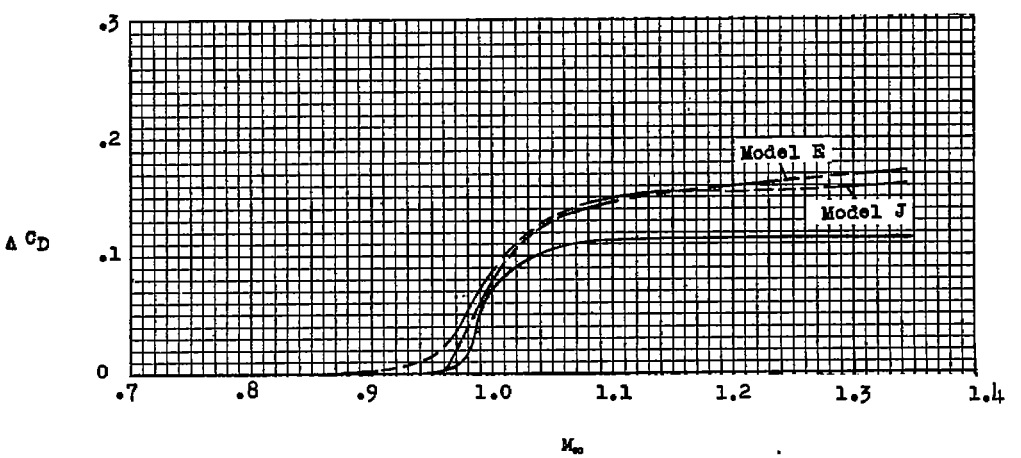

(b) Pressure drag.

Figure 18.- Comparison of total drag and pressure drag coefficients of fineness-ratio-7.00 canopies with flat and vee windshields at mid-position (x/l = 0.50) on the indented fuselage.